Title

Rapid homeostasis by disinhibition during whisker map plasticity

Journal

Proceedings of the National Academy of Sciences of the United States of America, 111(4)

ISSN

0027-8424

Authors

Li, Lu
Gainey, Melanie A
Goldbeck, Joseph E
et al.

Publication Date

2014-01-28

DOI

10.1073/pnas.1312455111

Peer reviewed

Rapid homeostasis by disinhibition during whisker map plasticity

Lu Li[1], Melanie A. Gainey, Joseph E. Goldbeck, and Daniel E. Feldman[2]

Department of Molecular and Cellular Biology and Helen Wills Neuroscience Institute, University of California, Berkeley, CA 94720

Edited by Michael Merzenich, Brain Plasticity Institute, San Francisco, CA, and approved December 18, 2013 (received for review July 1, 2013)

How homeostatic processes contribute to map plasticity and stability in sensory cortex is not well-understood. Classically, sensory deprivation first drives rapid Hebbian weakening of spiking responses to deprived inputs, which is followed days later by a slow homeostatic increase in spiking responses mediated by excitatory synaptic scaling. Recently, more rapid homeostasis by inhibitory circuit plasticity has been discovered in visual cortex, but whether this process occurs in other brain areas is not known. We tested for rapid homeostasis in layer 2/3 (L2/3) of rodent somatosensory cortex, where D-row whisker deprivation drives Hebbian weakening of whisker-evoked spiking responses after an unexplained initial delay, but no homeostasis of deprived whisker responses is known. We hypothesized that the delay reflects rapid homeostasis through disinhibition, which masks the onset of Hebbian weakening of L2/3 excitatory input. We found that deprivation (3 d) transiently increased whisker-evoked spiking responses in L2/3 single units before classical Hebbian weakening (≥5 d), whereas whisker-evoked synaptic input was reduced during both periods. This finding suggests a transient homeostatic increase in L2/3 excitability. In whole-cell recordings from L2/3 neurons in vivo, brief deprivation decreased whisker-evoked inhibition more than excitation and increased the excitation–inhibition ratio. In contrast, synaptic scaling and increased intrinsic excitability were absent. Thus, disinhibition is a rapid homeostatic plasticity mechanism in rodent somatosensory cortex that transiently maintains whisker-evoked spiking in L2/3, despite the onset of Hebbian weakening of excitatory input.

conductance

During deprivation-induced sensory map plasticity in cerebral cortex, changes in sensory input trigger both homeostatic plasticity mechanisms that maintain stable cortical firing rates and Hebbian mechanisms, in which inactive inputs lose (and active inputs gain) representation in sensory maps (1). Diverse mechanisms for homeostasis exist, including synaptic scaling (2–4), plasticity of intrinsic excitability (5, 6), and changes in sensory-evoked inhibition and excitation–inhibition (E-I) ratio (7–11). How homeostatic and Hebbian mechanisms interact to control map stability and plasticity remains unclear.

One key unknown is the relative dynamics of homeostatic and Hebbian plasticity. Homeostasis mediated by synaptic scaling is slow, occurring over hours in vitro and days in vivo. This process is evident in visual cortex, where eyelid closure during the critical period classically drives Hebbian weakening of closed eye spiking responses (after 2 d of deprivation) followed several days later by a slower homeostatic increase in visual responses (12, 13) mediated by excitatory synaptic scaling (3, 14, 15). We investigated whether more rapid forms of homeostasis also exist that shape the earliest stages of cortical plasticity. Recent results in visual cortex show that eyelid closure rapidly weakens inhibitory circuits (within 1 d), and this process increases network excitability and, therefore, is an initial homeostatic response to deprivation (10, 16). This disinhibition correlates with rapid structural plasticity in inhibitory axons and dendrites (17) and is mediated by a reduction in excitatory drive to parvalbumin-positive interneurons (10). Whether rapid homeostasis by disinhibition or other mechanisms is a general feature of cortical plasticity outside the visual cortex is unknown. Theoretical work shows that rapid homeostasis by inhibitory and/or intrinsic plasticity can guide development of realistic sensory tuning and sparse sensory coding in cortical networks, suggesting broad relevance (18).

We tested for rapid homeostasis during the onset of whisker map plasticity in the rodent primary somatosensory (S1) cortex, a major model of cortical plasticity. Each cortical column in the S1 whisker map corresponds to one facial whisker, termed its principal whisker (PW). Trimming or plucking a subset of whiskers in young adults weakens spiking responses to deprived PWs in layer 2/3 (L2/3) of deprived columns (19, 20). This process is mediated by Hebbian synaptic weakening at L4–L2/3 and L2/3–L2/3 excitatory synapses (21–23). No homeostatic restoration or strengthening of deprived whisker responses is known. However, PW response weakening is often preceded by an unexplained initial delay of ∼7 d, in which deprived whisker-evoked spiking responses remain stable (24, 25). We hypothesized that this initial delay reflects not a lack of plasticity but rapid homeostasis that (*i*) masks initial Hebbian weakening of L2/3 excitatory input and (*ii*) is mediated by loss of inhibition and/or increased intrinsic excitability in L2/3 neurons. Such rapid homeostasis would be a unique component of whisker map plasticity.

Results

Early Homeostatic Phase of Plasticity Precedes Classical Hebbian Depression. To detect a rapid homeostatic phase of plasticity, we measured whisker-evoked extracellular spiking in urethane-anesthetized rats following increasing durations of D-row whisker deprivation and in age-matched whisker-intact controls (Fig. 1). D-row deprivation was begun at postnatal day (P)21 ± 1

Significance

Neurons exhibit distinct homeostatic and Hebbian forms of plasticity that stabilize firing rate and adaptively alter synaptic input patterns, respectively. How these mechanisms are recruited in response to sensory experience in vivo is unclear. We studied plasticity in rodent somatosensory cortex, where the neural map of the whiskers adaptively changes to reflect sensory statistics but only after a prominent initial delay. By recording synaptic excitation and inhibition in vivo, we found that the delay reflects not a lack of plasticity but a rapid homeostasis, in which inhibition is powerfully reduced to offset the initial Hebbian reduction of whisker-evoked excitation. Thus, rapid homeostasis by disinhibition stabilizes the whisker map and precedes classical whisker map plasticity.

Author contributions: D.E.F. designed research; L.L., M.A.G., and J.E.G. performed research; L.L., M.A.G., J.E.G., and D.E.F. analyzed data; and L.L. and D.E.F. wrote the paper.

The authors declare no conflict of interest.

This article is a PNAS Direct Submission.

[1]Present address: Allen Institute for Brain Science, Seattle, WA 98103.

[2]To whom correspondence should be addressed. E-mail: dfeldman@berkeley.edu.

This article contains supporting information online at www.pnas.org/lookup/suppl/doi:10.1073/pnas.1312455111/-/DCSupplemental.

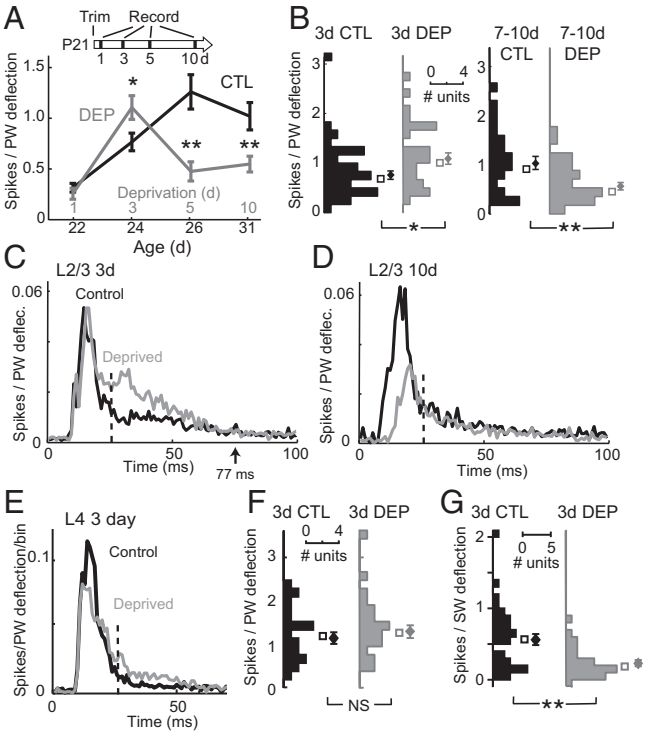

Fig. 1. Whisker deprivation causes a transient, compensatory increase in L2/3 sensory responses before classical Hebbian depression. (*A*) PW-evoked spikes (mean ± SEM) for L2/3 single units in normal rats and rats with D-row whisker deprivation from P21. Three-day deprivation transiently increased responses to the deprived PW before classical Hebbian depression. (*B*) Distribution of response magnitude for L2/3 units after 3 or 7–10 d of deprivation as well as in age-matched controls. (*C* and *D*) Population poststimulus time histogram (1-ms time bins) for PW responses of all L2/3 single units after 3 or 7–10 d of deprivation and in age-matched controls. Dashed lines (25 ms) separate early from late response epoch. (*E*) Population poststimulus time histogram for L4 single units after 3 d of deprivation. (*F*) Distribution of PW response magnitude for L4 units after 3 d of deprivation. (*G*) Effect of 3 d of deprivation on spiking responses to spared surround whiskers (SWs) for L2/3 units. $*P < 0.05$; $**P < 0.01$. NS, not significant.

(mean ± SD). In control rats, L2/3 spiking responses to PW deflection increased from P22 (the first day of recording) to P31, reflecting circuit maturation. In deprived rats, 3 d of deprivation caused a previously unknown 46% increase in deprived PW responses in L2/3 of D columns of deprived rats (mean age = P24) versus age-matched controls [control (CTL): 0.77 ± 0.09 spikes/stimulus, $n = 42$ units; deprived (DEP): 1.11 ± 0.12 spikes/stimulus, $n = 30$ units; $P < 0.02$, two-tailed t test]. This increase occurred specifically in long latency spikes (25–77 ms) (Fig. S1 *A* and *B*), and spontaneous firing rate was unaffected (CTL: 1.84 ± 0.26 spikes/s; DEP: 1.66 ± 0.21 spikes/s; $P = 0.59$), suggesting a possible reduction in PW-evoked inhibition. The increased spiking was replaced by classical Hebbian depression at 5–10 d of deprivation (5 d CTL: 1.26 ± 0.17 spikes/stimulus, $n = 23$; DEP: 0.48 ± 0.10 spikes/stimulus, $n = 25$; $P < 0.01$; 10 d CTL: 1.02 ± 0.14 spikes/stimulus, $n = 24$; DEP: 0.55 ± 0.08 spikes/stimulus, $n = 30$; $P < 0.01$) (Fig. 1 *A*–*D*). All recording sites were matched in columnar location and depth, and the greatest response enhancement at 3 d was observed in middle and deep L2/3 (Fig. S1). L4 responses were unaffected (3 d CTL: 1.14 ± 0.13 spikes/stimulus, $n = 21$; DEP: 1.32 ± 0.16 spikes/stimulus, $n = 23$; $P = 0.38$) (Fig. 1 *E* and *F*). Thus, deprivation drives an apparent compensatory enhancement of L2/3 spiking responses to the deprived PW before classical Hebbian weakening. At 3 d, responses to spared surround whiskers were reduced rather than enhanced, indicating whisker-specific rather than global homeostatic plasticity (Fig. 1*G*).

To confirm that Hebbian response weakening is absent at 3 d of deprivation, we recorded whisker responses at 3 vs. 7–10 d using intrinsic signal optical imaging (ISOI), which is an indirect hemodynamic measure of L2/3 activity (20, 26). ISOI avoids potential single-unit selection bias but has relatively low sensitivity for small changes in neural activity. D whisker-evoked peak signal intensity and cortical response area were unaltered by 3 d of deprivation vs. age-matched controls (DEP: $n = 21$ rats; CTL: $n = 32$; $P = 0.57$, t test) but reduced after 7–10 d of deprivation (DEP: $n = 23$; CTL: $n = 34$; $P < 0.0003$) (Fig. 2 *A*–*C*). The ratio of D1 response area to the mean of E1 and C1 responses areas within each animal (which controls for cross-animal differences in overall responsiveness) was not altered at 3 d but sharply reduced at 7–10 d (Fig. S2). Together with the single-unit data, this finding indicates that cortical responses are generally preserved at 3 d and decrease at 7–10 d of deprivation, as observed in adult rats and mice (24). ISOI did not detect the increase in late spiking at 3 d of deprivation, reflecting either low sensitivity or offsetting effects of the subthreshold contribution to the intrinsic signal.

Reduced Whisker-Evoked Local Field Potential During the Early Homeostatic Phase. To probe the basis for response enhancement at 3 d, we measured whisker-evoked local field potentials (wLFPs) in L2/3, which primarily reflect sensory-evoked subthreshold synaptic input (27). Current source density analysis from a 16-site linear probe confirmed that the wLFP in mid-L2/3 (400-μm depth) reflects a discrete L2/3 current sink (Fig. S3*A*). We compared L2/3 wLFPs between deprived D and spared B columns in D row-deprived rats. After 3 d of deprivation, wLFP amplitude was 43 ± 3% lower in D than B columns (D: −369 ± 45 μV; B: −602 ± 63 μV, $n = 9$ penetrations each; $P < 0.01$, two-tailed t test) (Fig. 2 *D* and *E*). This reduction occurred between 1 and 3 d of deprivation, and D-column wLFPs remained stably smaller after 5 and 10 d of deprivation (5 d D: −357 ± 58, $n = 9$; B: −533 ± 29 μV, $n = 6$; $P < 0.04$; 10 d D: −437 ± 43, $n = 8$; B: −620 ± 51, $n = 7$; $P < 0.02$). The same pattern was observed for wLFP initial slope (Fig. S2) and wLFP ratio (D/B column)

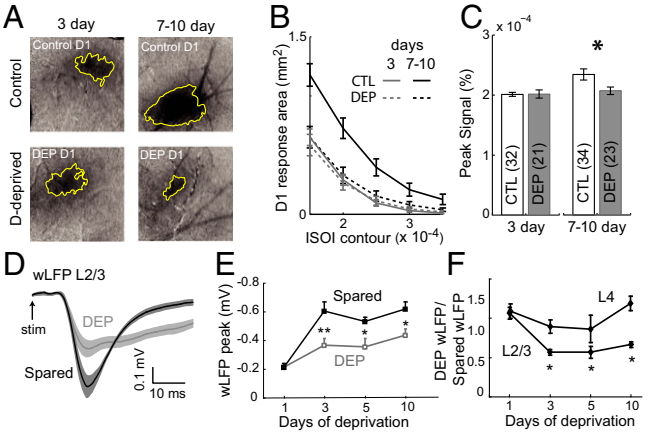

Fig. 2. Stable ISOI but reduced wLFPs during the 3-d homeostatic phase of plasticity. (*A*) Example intrinsic signal images (3 × 3-mm field) during D1 whisker deflection for 3- and 7-d deprived animals and age-matched controls. (*B*) Mean D1 whisker response area for each condition. (*C*) Peak intrinsic signal (mean of four neighboring pixels) for each condition. (*D*) Mean wLFP waveforms for all L2/3 recordings in 3-d deprived (gray) and spared (black) columns. Shading is SEM. (*E*) L2/3 wLFP peak amplitude (mean ± SEM) for deprived and spared columns at varying deprivation durations. (*F*) wLFP amplitude ratio (deprived/spared column within each animal) for L2/3 and L4 wLFPs. $*P < 0.05$. $**P < 0.01$.

computed in single animals (Fig. 2*F*). In contrast, L4 wLFPs were not significantly affected (Fig. 2*F*). These findings suggest that 3 d of deprivation weakens PW-evoked synaptic drive to L2/3, even as PW-evoked spiking is increased, suggestive of a homeostatic increase in L2/3 excitability.

PW-Evoked Excitation and Inhibition. To directly test how subthreshold synaptic input is altered by 3 d of deprivation, we measured whisker-evoked synaptic currents in single L2/3 neurons using blind whole-cell voltage clamp recordings in vivo (28). Recordings were targeted by intrinsic signal optical imaging to deprived D1 or D2 columns in deprived animals and control D1, D2, E1, C1, and δ-columns in whisker-intact littermates. Recordings were made in L2/3 at 396 ± 10 μm (range = 273–590 μm) subpial depth, with Cs gluconate, N-(2,6-dimethylphenylcarbamoylmethyl)triethylammonium (QX-314) bromide, and 1,2-bis(o-aminophenoxy)ethane- N,N,N′,N′-tetraacetic acid (BAPTA) to promote voltage clamp. We presume that most cells are pyramidal neurons, which are 90% of L2/3 neurons in this depth range (29). For each cell, we determined the PW and measured PW-evoked postsynaptic currents (wPSCs) at multiple holding potentials (−90 to + 30 mV) using a standardized whisker stimulus (2° up–down deflection, 550°/s) (Fig. S4). Inclusion criteria included linear current–voltage (I–V) relationship (Fig. S4) and initial resting membrane potential (Vrest) of < −60 mV. We estimated whisker-evoked total synaptic conductance (Gtotal), inhibitory synaptic conductance (Gin), and excitatory synaptic conductance (Gex) based on the parallel conductance equation using standard methods (30, 31). Conductance waveforms were calculated from 0 to 77 ms poststimulus, where I–V relations were most consistently linear. Because of incomplete dendritic voltage clamp (32), these measurements reflect apparent synaptic conductance at the soma. We showed previously that this method (used in S1 slices) detects the majority of L4-evoked excitation and somatic inhibition in L2/3 pyramidal cells (33).

We first compared 3-d deprived cells with age-matched controls (Fig. 3). In control cells (n = 19; P24 ± 1), PW-evoked wPSCs and apparent synaptic conductances were small (median peak Gtotal = 0.92 nS; median peak Gex = 0.67 nS; median peak Gin = 0.42 nS), paralleling the weak spiking responses in L2/3 at this age (34). Gex waveforms often showed slow dynamics, which may reflect a predominance of recurrent excitation or NMDA receptor currents. Three days of deprivation (n = 19 cells; P24 ± 1) reduced PW-evoked Gtotal, Gex, and Gin relative to control animals (Fig. 3 and Table 1). This reduction was true for both integrated conductance (0–77 ms; reduced 51.5%, 55.0%, and 81.4% below control for Gtotal, Gex, and Gin, respectively) and peak conductance (60.8%, 53.7%, and 71.4% for Gtotal, Gex, and Gin, respectively). Thus, 3 d of deprivation depressed both whisker-evoked excitation and whisker-evoked inhibition in L2/3 neurons. Recording depth, input resistance (Rinput), and series resistance (Rseries) did not differ between control and deprived cells (Table S1), but Vrest was slightly elevated in deprived cells (see below).

To examine effects on E-I ratio, we plotted peak Gex vs. peak Gin for each cell and observed an increase in excitation relative to inhibition after deprivation (Fig. 4*A*). To quantify this effect, we calculated Gex fraction [Gex/(Gex + Gin)] for each individual neuron (Fig. 4*B*). Gex fraction calculated from integrated conductance was significantly increased after 3 d of deprivation relative to age-matched controls [median (25th, 75th percentile); CTL: 0.56 (0.42, 0.81); DEP: 0.85 (0.65, 0.94); P = 0.015, Wilcoxon rank test]. Gex fraction calculated from peak conductance also increased [CTL: 0.57 (0.43, 0.67); DEP: 0.77 (0.61, 0.88); P = 0.009]. When Gex fraction was calculated millisecond by millisecond during the response, a significant increase was found from 25 to 77 ms poststimulus (the same late epoch when whisker-evoked spikes were increased) (Fig. 4*C*). Thus, deprivation rapidly reduced whisker-evoked Gex in deprived columns but reduced Gin even more strongly, leading to an increase in E-I ratio. This effect, which co-occurred with increased whisker-evoked spiking, indicates rapid disinhibition, which would function to homeostatically increase network excitability after loss of PW-evoked sensory drive (9).

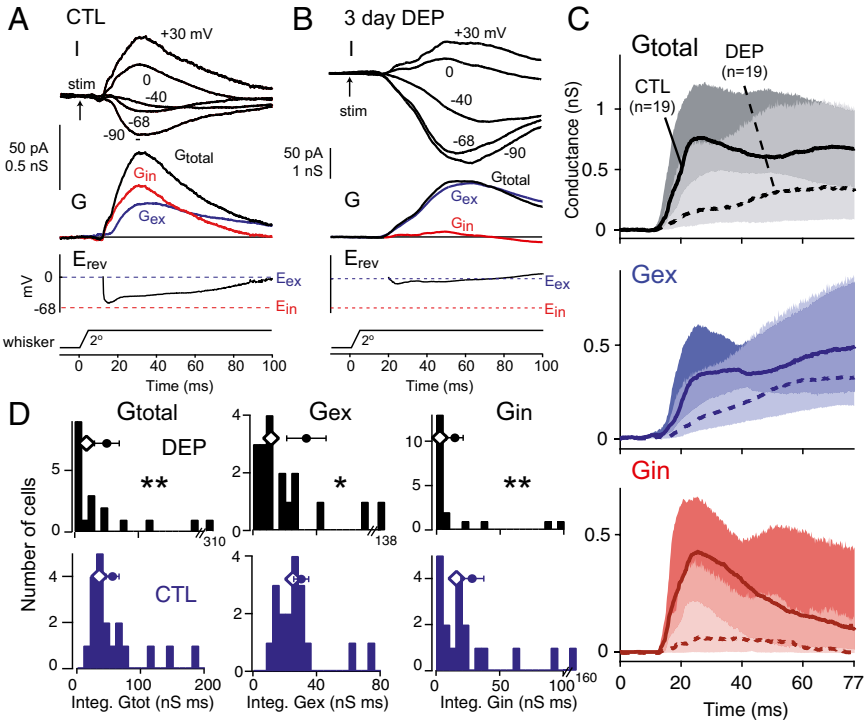

Fig. 3. Three-day deprivation decreases whisker-evoked inhibition and excitation onto L2/3 neurons in vivo. (*A* and *B*) Example cells from a control rat (P25) and a 3-d deprived rat (P24). Erev, apparent reversal potential during the response relative to excitatory and inhibitory reversal potentials (Eex and Ein, respectively); G, synaptic conductance; I, whisker-evoked current at specified holding potential after stimulus onset (arrow). (*C*) Population Gtotal, Gin, and Gex from 3-d deprived rats and age-matched controls. Lines are median, and shading shows 25th to 75th percentiles. (*D*) Distribution of integrated Gtotal, Gex, and Gin for all cells. Diamonds show median. Circles and bars are mean ± SEM. $P < 0.05$; $^{**}P < 0.01$.

Table 1. PW-evoked synaptic conductances in L2/3 neurons

Condition	Cells	Measurement	Gtotal (nS)	Gex (nS)	Gin (nS)
CTL P23–P25	19	Peak (nS)	0.92 (0.72, 1.6)	0.67 (0.45, 1.0)	0.42 (0.30, 0.88)
		Integral (nS × ms)	35.2 (29.2, 67.9)	25.3 (18.1, 34.4)	16.1 (6.6, 32.7)
DEP 3 d (P23–P25)	19	Peak (nS)	0.36 (0.14, 1.1)*	0.31 (0.20, 0.89)†	0.12 (0.05, 0.43)*
		Integral (nS × ms)	7.1 (5.0, 51)*	11.4 (7.0, 34)†	3.0 (0.92, 13.4)*
CTL P27–P32	12	Peak (nS)	1.3 (0.88, 4.6)	0.73 (0.46, 2.1)	1.0 (0.44, 3.0)
		Integral (nS × ms)	60.4 (36.9, 200)	25.4 (20.3, 70.4)	37.8 (13.7, 138)
DEP 7–10 d (P27–P32)	18	Peak (nS)	0.73 (0.22, 1.9)†	0.50 (0.17, 1.3)‡	0.36 (0.07, 0.82)*
		Integral (nS × ms)	28.9 (7.0, 83.5)†	16.1 (5.7, 51.2)‡	8.3 (0.91, 29.7)*

*Significantly different from CTL: $P < 0.01$.
†Significantly different from CTL: $P < 0.05$.
‡Trend: $P < 0.07$ (Wilcoxon rank test).

To better characterize the deprivation effect, we separately analyzed early (0–25 ms) and late (25–77 ms) epochs in the PW response (Fig. S5). In the early epoch, deprivation reduced integrated Gex and Gin similarly (median conductance value reduced to 0.26 and 0.09 of control, respectively; $P < 0.01$), and Gex fraction was unchanged [CTL: 0.48 (0.37, 0.56); DEP: 0.55 (0.34, 0.81); $P = 0.16$]. In the late epoch, deprivation reduced Gex modestly (0.60 of control; $P < 0.05$) and Gin substantially (0.21 of control; $P < 0.01$), and Gex fraction was increased [CTL: 0.58 (0.45, 0.83); DEP: 0.86 (0.68, 0.97); $P = 0.014$]. Thus, both excitation and inhibition were reduced throughout the response, with a nonsignificant trend for greater reduction of early vs. late Gex ($P = 0.10$). The early epoch showed parallel reduction of Gex and Gin, which was associated with no change in PW-evoked spiking, whereas the late epoch showed a preferential reduction in Gin, which was associated with increased PW-evoked spiking.

Disinhibition Persists After 7 d of Deprivation. Disinhibition could occur transiently during the early homeostatic phase of plasticity or persist during the later Hebbian weakening phase of plasticity. To distinguish these possibilities, we measured whisker-evoked synaptic conductance after 7–10 d of deprivation vs. in age-matched whisker-intact control rats (P27–P32) (Fig. S6). In control animals ($n = 12$ cells), Gtotal, Gex, and Gin were slightly but not significantly greater than at P24 ± 1 ($P > 0.07$) (Table 1). In rats with 7–10 d of deprivation ($n = 18$ cells), PW-evoked Gtotal and Gin were reduced (integral: 52.2% and 78.0% less than age-matched controls; peak: 43.8% and 64%; $P < 0.05$), and there was a trend for reduction of Gex (integral: 36.6% less then control; peak: 31.5%; $P < 0.07$) (Table 1). The effect on Gex fraction was similar to 3 d of deprivation but only significant at trend level (Gex from integrated conductance: $P = 0.052$; from peak: $P = 0.073$) (Fig. S6*D*). Gex fraction calculated millisecond by millisecond during the whisker response showed significant disinhibition late in the response, again similar to 3 d of deprivation (Fig. S6*E*). Recording depth, Rinput, and Rseries were not different between deprived and control cells (Table S1). Vrest was unchanged after 7–10 d of deprivation (CTL: −71.2 ± 0.7 mV, $n = 24$ cells; DEP: −70.4 ± 1.2 mV, $n = 18$ cells; $P = 0.21$, Wilcoxon rank test). Thus, disinhibition was largely sustained during the later Hebbian phase of plasticity, and both early homeostatic and later Hebbian phases of plasticity involved weakening of both excitation and inhibition. Although the relative latency of Gex and Gin strongly impacts sensory-evoked spiking (35), deprivation did not alter the relative timing of Gex vs. Gin onset (mean Gex − Gin latency difference, CTL: 1.9 ± 0.8 ms; DEP: 2.3 ± 1.7 ms for 3 and 7–10 d data combined).

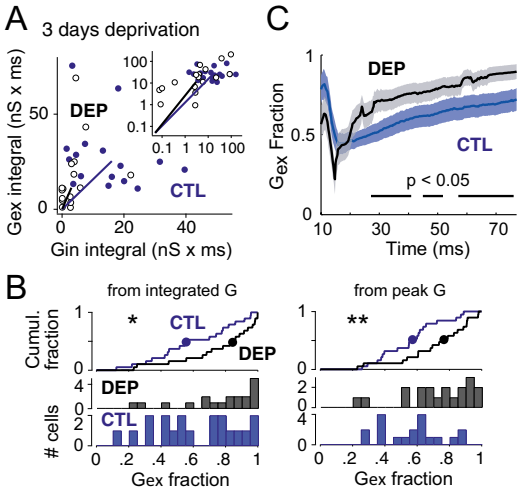

Fig. 4. Three-day deprivation increases E-I ratio. (*A*) Integrated Gex vs. Gin for each cell in 3-d deprived rats and age-matched controls. *Inset* shows full population on log scale, and the main plot shows all but the six largest conductance cells on linear scale for better visualization. Solid lines mark population medians. (*B*) Distribution of Gex fraction calculated from integrated and peak conductance values for each cell. Medians (circles) are marked on cumulative histograms (*Top*). (*C*) Moment by moment analysis of Gex fraction (1-ms bins) averaged across all cells. Bars indicate time periods when Gex fraction was significantly increased in deprived cells by running *t* test. $P < 0.05$; $^{**}P < 0.01$.

Synaptic Scaling and Intrinsic Excitability. To determine whether rapid homeostasis also involves synaptic scaling (2) or increased intrinsic excitability in L2/3 pyramidal cells (8), we made whole-cell recordings from visually identified L2/3 pyramidal cells in ex vivo S1 brain slices prepared from D row-deprived rats (onset: P19–P21, duration: 3 d) and age-matched, sham-deprived littermates. We targeted recordings to visualized D columns (21, 36). To examine synaptic scaling, AMPA receptor-mediated miniature excitatory postsynaptic currents (mEPSCs; 200–300 per cell) were isolated using TTX (0.5 μM), picrotoxin (100 μM), and D-amino-5-phosphonovaleric acid (50 μM) and recorded at 30 °C at −90 mV. mEPSC amplitude and frequency distributions were identical between D columns in deprived ($n = 8$ cells) and sham ($n = 10$ cells) slices ($P = 0.28$ and $P = 0.92$, respectively), and mEPSC kinetics were also identical (Fig. 5*A*). Example mEPSCs are shown in Fig. S7. Identical results were obtained in additional cells at 22–25 °C ($n = 9$ deprived and 10 sham cells) (Fig. S7). Thus, synaptic scaling was not detectable with brief deprivation. NMDA current kinetics were also unchanged (Fig. S7).

Three-day deprivation depolarized Vrest for both L2/3 neurons in vivo (CTL: −70.1 ± 0.9 mV, $n = 35$ cells; DEP: −67 ± 1.1 mV, $n = 26$ cells; $P = 0.016$, Wilcoxon rank test) and L2/3 pyramidal cells in D columns in brain slices, which were measured either with synaptic transmission intact (SHAM: −74.0 ± 0.9 mV, $n = 19$ cells; DEP: −70.7 ± 1.0 mV, $n = 22$ cells; $P < 0.02$) or

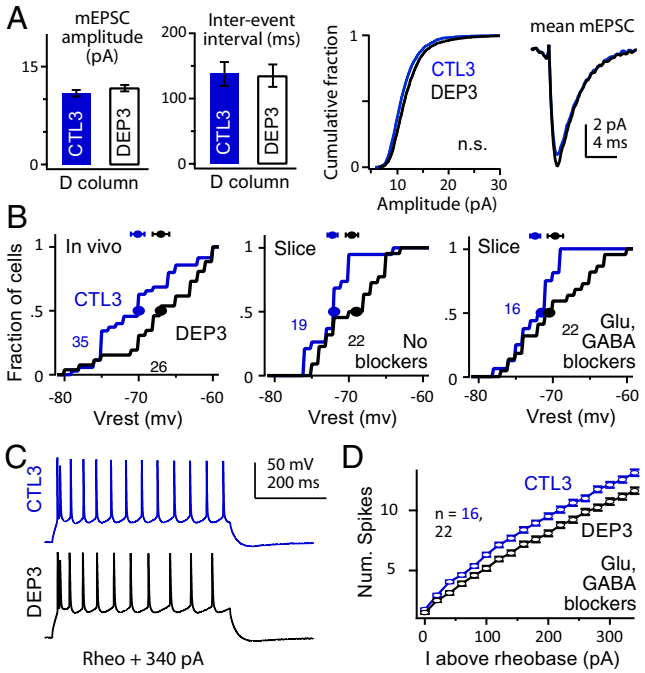

Fig. 5. Lack of synaptic scaling and reduction in intrinsic excitability. (*A*) mEPSCs are not altered in D columns by 3-d deprivation. From left to right, mean mEPSC amplitude, mean interevent interval, cumulative amplitude distribution, and mean mEPSC waveforms ($n = 10$ control and $n = 8$ deprived cells) are shown. (*B*) Cumulative distribution and medians (circles) of Vrest for (*Left*) L2/3 neurons in vivo and visually identified L2/3 pyramidal cells in D column of S1 slices (*Center*) without and (*Right*) with synaptic blockers. Points and error bars show mean ± SEM. (*C* and *D*) Example spike trains and relationship between firing rate and injected current for sham D and deprived D columns, measured in synaptic blockers.

in the presence of synaptic blockers of fast GABAergic and glutamatergic transmission (picrotoxin, 100 μM; 2,3-dioxo-6-nitro-1,2,3,4-tetrahydrobenzo[f]quinoxaline-7-sulfonamide, 10 μM; D-APV, 50 μM; SHAM: −72.4 ± 0.68 mV, $n = 16$ cells; DEP: −69.4 ± 1.1 mV, $n = 22$ cells; $P = 0.04$) (Fig. 5*B*). Deprivation did not alter input resistance (this measurement and all subsequent measurements in synaptic blockers: SHAM: 74.8 ± 4.7 MΩ, $n = 16$ cells; DEP: 75.2 ± 5.2 MΩ, $n = 22$ cells; $P = 0.95$, t test) or Ih as measured by Vm sag ratio ($P = 0.92$) (Fig. S7).

Despite elevated Vrest, the somatic current required to elicit a single spike (rheobase) was unchanged after deprivation (SHAM: 251.2 ± 14 pA, $n = 13$ cells; DEP: 256.9 ± 14 pA, $n = 12$ cells; $P = 0.77$). Above rheobase, however, the relationship between firing rate and injected current was depressed in deprived D columns relative to sham D columns (ANOVA $P = 0.004$) (Fig. 5 *C* and *D*). Reduced intrinsic excitability has also been observed previously after whisker deprivation (37) and peripheral denervation (38). The reduced firing rate was associated with increased spike width (ANOVA $P = 0.012$) but no change in spike threshold (Fig. S7) or amplitude of afterhyperpolarization after each spike in the train ($P = 0.7$).

Thus, brief deprivation did not induce synaptic scaling but did induce three rapid effects in L2/3 of deprived columns: a substantial reduction in whisker-evoked inhibition, a smaller reduction in excitation, and a modest reduction in intrinsic spiking excitability.

Discussion

Prior studies reported an unexplained delay (up to 7 d) between the onset of whisker row deprivation and the Hebbian loss of spiking responses to deflection of deprived whiskers (20, 24). Our results show that this delay represents not an absence of plasticity but a period of active homeostasis, in which network excitability is rapidly increased in L2/3 of deprived S1 columns to compensate for the Hebbian loss of whisker-evoked excitation. This homeostasis is substantial enough to maintain (and even slightly increase) whisker-evoked L2/3 firing rate and maintain normal spontaneous activity, despite a significant concurrent reduction in synaptic excitation in L2/3. Thus, rapid homeostasis maintains constant cortical activity for several days after altered sensory use, as proposed theoretically (1).

Brief (3-d) deprivation weakened whisker-evoked inhibition more than excitation, thus increasing E-I ratio in L2/3 neurons. Thus, disinhibition is a major component of rapid homeostasis in S1. Disinhibition and other inhibitory circuit modifications are well-known after sustained deprivation in visual cortex (7, 8, 11, 39–41) and S1 (33, 42–44). Rapid disinhibition (i.e., before the onset of classical Hebbian response plasticity) is proposed as an early step in lesion-induced adult plasticity in S1 (45) and tone-shock conditioning in auditory cortex (46), and it was recently observed in visual cortex after visual deprivation (10, 16). Our results show that this same phenomenon acts to maintain stable spiking in S1. Disinhibition was previously observed in S1 in cortical columns corresponding to spared whiskers, where it promotes subsequent steps in whisker map plasticity (9), but the current results demonstrate disinhibition in deprived columns, where it mediates sensory response homeostasis. The rapid functional reduction in sensory-evoked inhibition is consistent with rapid pruning of GABAergic neuron dendrites and axons after sensory deprivation or a delay in GABAergic synapse maturation (17, 47, 48).

A likely circuit locus for disinhibition in L2/3 of deprived S1 columns is within the local L2/3 recurrent network, where sustained deprivation (>5 d) is known to weaken recurrent inhibition more than excitation (43). In contrast, feedforward L4–L2/3 excitation and inhibition are weakened equally, on average, by sustained deprivation (33). Preferential disinhibition in the recurrent network would explain the current finding that whisker-evoked Gex fraction and spiking are selectively increased at long poststimulus latencies (Figs. S1 and S6). In visual cortex, rapid disinhibition is mediated by reduced excitation onto L2/3 parvalbumin-positive interneurons (10, 16), which may also be the case in S1 (33).

Brief deprivation modestly decreased intrinsic excitability in L2/3 pyramidal cells, despite elevating Vrest. These effects were small (5–10% change relative to controls) relative to the reduction in whisker-evoked inhibition (~70–80% reduced from controls), suggesting that disinhibition is the dominant effect. Homeostatic synaptic scaling was absent at 3 d of deprivation, consistent with the relatively slow dynamics of scaling observed in V1 (4, 49). How the initial homeostatic increase in whisker-evoked spiking responses after deprivation is transformed to subsequent Hebbian depression is unclear, because Gex and Gin were reduced similarly after 3 vs. 7–10 d of deprivation (Fig. S6). Possibilities include additional reduction of intrinsic excitability at 7–10 d and changes in distal excitatory or inhibitory inputs that could not be detected in our whole-cell recordings in vivo.

We note several functional advantages of disinhibition as a mechanism of network homeostasis. First, disinhibition will achieve higher network firing rates with less total synaptic current than global homeostatic strengthening of excitatory synapses and thus, may be more efficient metabolically. Second, because inhibitory neurons innervate nearly all local pyramidal cells (50, 51), decreased excitatory drive to a few interneurons may regulate an entire local network uniformly. Third, disinhibition powerfully promotes dendritic depolarization and spiking and therefore, may gate subsequent Hebbian synaptic potentiation during map plasticity (9, 10). Indeed, this gating of plasticity, rather than acute restoration of sensory representation, may be the primary role of disinhibition (52). Fourth, in cases where specific interneurons are tuned to specific sensory features (53), feature-specific homeostasis could be implemented by disinhibition within the specific

interneuron class. Consistent with this idea, 3 d of deprivation homeostatically increased spiking responses to deprived PWs but reduced responses to spared surround whiskers (Fig. 1*G*). This finding is consistent with prior results (24) and not consistent with global homeostasis mediated by synaptic scaling (2, 13).

Materials and Methods

Long–Evans rats (P19–P36) were used. Procedures were approved by the University of California at Berkeley Animal Care and Use Committee and meet National Institutes of Health guidelines. Whiskers (D1–D6 and γ) were deprived unilaterally by trimming, and control animals were sham-trimmed littermates. In vivo recording was performed under urethane anesthesia. Standardized whisker deflections were applied 3 mm from the face in both control and deprived rats. Single-unit LFP and whole-cell recordings were targeted by ISOI to the center of a D1 whisker functional column. Whole-cell recording in vivo used internal with cesium, QX-314, and BAPTA, and Rseries was not corrected. Whisker-evoked excitatory and inhibitory synaptic conductances were estimated from wPSCs at five holding potentials using standard methods (31, 54). Slice physiology was performed in across-row S1 slices that allow visualization of A–E whisker columns (21, 36). Recordings were made from visually identified L2/3 pyramidal neurons in D-barrel columns. Rseries was compensated for by voltage clamp experiments. Numbers are mean ± SE or median (25th, 75th percentile). Conductance values were nonnormally distributed and compared by nonparametric tests. Detailed methods are in *SI Materials and Methods*.

ACKNOWLEDGMENTS. We thank Brooke Angel for analysis, and M. R. DeWeese and laboratory members for comments. This work was supported by National Institutes of Health Grants R01NS073912 and R01NS046652-07A1.

1. Turrigiano GG, Nelson SB (2004) Homeostatic plasticity in the developing nervous system. *Nat Rev Neurosci* 5(2):97–107.
2. Turrigiano GG, Leslie KR, Desai NS, Rutherford LC, Nelson SB (1998) Activity-dependent scaling of quantal amplitude in neocortical neurons. *Nature* 391(6670): 892–896.
3. Kaneko M, Stellwagen D, Malenka RC, Stryker MP (2008) Tumor necrosis factor-alpha mediates one component of competitive, experience-dependent plasticity in developing visual cortex. *Neuron* 58(5):673–680.
4. Desai NS, Cudmore RH, Nelson SB, Turrigiano GG (2002) Critical periods for experience-dependent synaptic scaling in visual cortex. *Nat Neurosci* 5(8):783–789.
5. Aizenman CD, Akerman CJ, Jensen KR, Cline HT (2003) Visually driven regulation of intrinsic neuronal excitability improves stimulus detection in vivo. *Neuron* 39(5): 831–842.
6. Breton J-D, Stuart GJ (2009) Loss of sensory input increases the intrinsic excitability of layer 5 pyramidal neurons in rat barrel cortex. *J Physiol* 587(Pt 21):5107–5119.
7. Maffei A, Nelson SB, Turrigiano GG (2004) Selective reconfiguration of layer 4 visual cortical circuitry by visual deprivation. *Nat Neurosci* 7(12):1353–1359.
8. Maffei A, Turrigiano GG (2008) Multiple modes of network homeostasis in visual cortical layer 2/3. *J Neurosci* 28(17):4377–4384.
9. Gambino F, Holtmaat A (2012) Spike-timing-dependent potentiation of sensory surround in the somatosensory cortex is facilitated by deprivation-mediated disinhibition. *Neuron* 75(3):490–502.
10. Kuhlman SJ, et al. (2013) A disinhibitory microcircuit initiates critical-period plasticity in the visual cortex. *Nature* 501(7468):543–546.
11. Ma W-P, Li Y-T, Tao HW (2013) Downregulation of cortical inhibition mediates ocular dominance plasticity during the critical period. *J Neurosci* 33(27):11276–11280.
12. Frenkel MY, Bear MF (2004) How monocular deprivation shifts ocular dominance in visual cortex of young mice. *Neuron* 44(6):917–923.
13. Mrsic-Flogel TD, et al. (2007) Homeostatic regulation of eye-specific responses in visual cortex during ocular dominance plasticity. *Neuron* 54(6):961–972.
14. Gao M, et al. (2010) A specific requirement of Arc/Arg3.1 for visual experience-induced homeostatic synaptic plasticity in mouse primary visual cortex. *J Neurosci* 30(21):7168–7178.
15. Lambo ME, Turrigiano GG (2013) Synaptic and intrinsic homeostatic mechanisms cooperate to increase L2/3 pyramidal neuron excitability during a late phase of critical period plasticity. *J Neurosci* 33(20):8810–8819.
16. Hengen KB, Lambo ME, Van Hooser SD, Katz DB, Turrigiano GG (2013) Firing rate homeostasis in visual cortex of freely behaving rodents. *Neuron* 80(2):335–342.
17. Keck T, et al. (2011) Loss of sensory input causes rapid structural changes of inhibitory neurons in adult mouse visual cortex. *Neuron* 71(5):869–882.
18. Zylberberg J, Murphy JT, DeWeese MR (2011) A sparse coding model with synaptically local plasticity and spiking neurons can account for the diverse shapes of V1 simple cell receptive fields. *PLoS Comput Biol* 7(10):e1002250.
19. Glazewski S, Fox K (1996) Time course of experience-dependent synaptic potentiation and depression in barrel cortex of adolescent rats. *J Neurophysiol* 75(4):1714–1729.
20. Drew PJ, Feldman DE (2009) Intrinsic signal imaging of deprivation-induced contraction of whisker representations in rat somatosensory cortex. *Cereb Cortex* 19(2): 331–348.
21. Allen CB, Celikel T, Feldman DE (2003) Long-term depression induced by sensory deprivation during cortical map plasticity in vivo. *Nat Neurosci* 6(3):291–299.
22. Shepherd GMG, Pologruto TA, Svoboda K (2003) Circuit analysis of experience-dependent plasticity in the developing rat barrel cortex. *Neuron* 38(2):277–289.
23. Cheetham CEJ, Hammond MSL, Edwards CEJ, Finnerty GT (2007) Sensory experience alters cortical connectivity and synaptic function site specifically. *J Neurosci* 27(13): 3456–3465.
24. Jacob V, Petreanu L, Wright N, Svoboda K, Fox K (2012) Regular spiking and intrinsic bursting pyramidal cells show orthogonal forms of experience-dependent plasticity in layer V of barrel cortex. *Neuron* 73(2):391–404.
25. Li L, et al. (2009) Endocannabinoid signaling is required for development and critical period plasticity of the whisker map in somatosensory cortex. *Neuron* 64(4):537–549.
26. Grinvald A, Lieke E, Frostig RD, Gilbert CD, Wiesel TN (1986) Functional architecture of cortex revealed by optical imaging of intrinsic signals. *Nature* 324(6095):361–364.
27. Heynen AJ, Bear MF (2001) Long-term potentiation of thalamocortical transmission in the adult visual cortex in vivo. *J Neurosci* 21(24):9801–9813.
28. Margrie TW, Brecht M, Sakmann B (2002) In vivo, low-resistance, whole-cell recordings from neurons in the anaesthetized and awake mammalian brain. *Pflugers Arch* 444(4):491–498.
29. Meyer HS, et al. (2011) Inhibitory interneurons in a cortical column form hot zones of inhibition in layers 2 and 5A. *Proc Natl Acad Sci USA* 108(40):16807–16812.
30. Borg-Graham LJ, Monier C, Frégnac Y (1998) Visual input evokes transient and strong shunting inhibition in visual cortical neurons. *Nature* 393(6683):369–373.
31. Wehr M, Zador AM (2003) Balanced inhibition underlies tuning and sharpens spike timing in auditory cortex. *Nature* 426(6965):442–446.
32. Williams SR, Mitchell SJ (2008) Direct measurement of somatic voltage clamp errors in central neurons. *Nat Neurosci* 11(7):790–798.
33. House DRC, Elstrott J, Koh E, Chung J, Feldman DE (2011) Parallel regulation of feedforward inhibition and excitation during whisker map plasticity. *Neuron* 72(5): 819–831.
34. Brecht M, Roth A, Sakmann B (2003) Dynamic receptive fields of reconstructed pyramidal cells in layers 3 and 2 of rat somatosensory barrel cortex. *J Physiol* 553(Pt 1): 243–265.
35. Wilent WB, Contreras D (2005) Dynamics of excitation and inhibition underlying stimulus selectivity in rat somatosensory cortex. *Nat Neurosci* 8(10):1364–1370.
36. Finnerty GT, Roberts LS, Connors BW (1999) Sensory experience modifies the short-term dynamics of neocortical synapses. *Nature* 400(6742):367–371.
37. Maravall M, Stern EA, Svoboda K (2004) Development of intrinsic properties and excitability of layer 2/3 pyramidal neurons during a critical period for sensory maps in rat barrel cortex. *J Neurophysiol* 92(1):144–156.
38. Hickmott PW (2005) Changes in intrinsic properties of pyramidal neurons in adult rat S1 during cortical reorganization. *J Neurophysiol* 94(1):501–511.
39. Yazaki-Sugiyama Y, Kang S, Câteau H, Fukai T, Hensch TK (2009) Bidirectional plasticity in fast-spiking GABA circuits by visual experience. *Nature* 462(7270):218–221.
40. Gandhi SP, Yanagawa Y, Stryker MP (2008) Delayed plasticity of inhibitory neurons in developing visual cortex. *Proc Natl Acad Sci USA* 105(43):16797–16802.
41. Maffei A, Nataraj K, Nelson SB, Turrigiano GG (2006) Potentiation of cortical inhibition by visual deprivation. *Nature* 443(7107):81–84.
42. Jiao Y, Zhang C, Yanagawa Y, Sun Q-Q (2006) Major effects of sensory experiences on the neocortical inhibitory circuits. *J Neurosci* 26(34):8691–8701.
43. Shao YR, et al. (2013) Plasticity of recurrent l2/3 inhibition and gamma oscillations by whisker experience. *Neuron* 80(1):210–222.
44. Hickmott PW, Merzenich MM (2002) Local circuit properties underlying cortical reorganization. *J Neurophysiol* 88(3):1288–1301.
45. Tremere L, Hicks TP, Rasmusson DD (2001) Role of inhibition in cortical reorganization of the adult raccoon revealed by microiontophoretic blockade of GABA(A) receptors. *J Neurophysiol* 86(1):94–103.
46. Letzkus JJ, et al. (2011) A disinhibitory microcircuit for associative fear learning in the auditory cortex. *Nature* 480(7377):331–335.
47. Marik SA, Yamahachi H, McManus JNJ, Szabo G, Gilbert CD (2010) Axonal dynamics of excitatory and inhibitory neurons in somatosensory cortex. *PLoS Biol* 8(6):e1000395.
48. van Versendaal D, et al. (2012) Elimination of inhibitory synapses is a major component of adult ocular dominance plasticity. *Neuron* 74(2):374–383.
49. Goel A, Lee H-K (2007) Persistence of experience-induced homeostatic synaptic plasticity through adulthood in superficial layers of mouse visual cortex. *J Neurosci* 27(25):6692–6700.
50. Fino E, Yuste R (2011) Dense inhibitory connectivity in neocortex. *Neuron* 69(6): 1188–1203.
51. Packer AM, Yuste R (2011) Dense, unspecific connectivity of neocortical parvalbumin-positive interneurons: A canonical microcircuit for inhibition? *J Neurosci* 31(37): 13260–13271.
52. Sale A, et al. (2007) Environmental enrichment in adulthood promotes amblyopia recovery through a reduction of intracortical inhibition. *Nat Neurosci* 10(6):679–681.
53. Adesnik H, Bruns W, Taniguchi H, Huang ZJ, Scanziani M (2012) A neural circuit for spatial summation in visual cortex. *Nature* 490(7419):226–231.
54. Monier C, Fournier J, Frégnac Y (2008) In vitro and in vivo measures of evoked excitatory and inhibitory conductance dynamics in sensory cortices. *J Neurosci Methods* 169(2):323–365.